Available online at www.sciencedirect.com
SCIENCE DIRECT®
Coordination Chemistry Reviews 248 (2004) 1469–1478
COORDINATION CHEMISTRY REVIEWS
www.elsevier.com/locate/ccr

Review

Photo-sensitizing ruthenium complexes for solid state dye solar cells in combination with conducting polymers as hole conductors

Yasuteru Saito, Takahiro Azechi, Takayuki Kitamura, Yasuchika Hasegawa, Yuji Wada, Shozo Yanagida*

Material and Life Science, Graduate School of Engineering, Osaka University, Suita, Osaka 565-0871, Japan

Received 18 October 2003; accepted 30 March 2004
Available online 28 May 2004

Contents

Abstract

Pyrrole- or thiophene-bearing pyridine ligands were designed to synthesize ruthenium complexes with pyrrole or thiophene groups as sensitizing dye molecules. Solid state dye sensitized solar cells (sDSCs) were fabricated using the newly designed ruthenium complexes as sensitizers and conducting polymers, polypyrrole and poly(3,4-ethylenedioxythiophene) as solid-state hole transport materials. The polymers were introduced into the void of mesoporous dye sensitized TiO_2 electrodes by in situ chemical- and photo-electrochemical polymerization. Employment of the novel ruthenium dyes with pyrrole or thiophene groups in the ligand systems improved the photovoltaic performance of the sDSCs. Electronic communication at the interface between the new ruthenium dyes and the conducting polymer coupled with ionic liquids was found to contribute to the improved photovoltaic performance of sDSCs.

Keywords: Dye sensitization; Conducting polymer; Polypyrrole; Poly(3,4-ethylenedioxythiophene); Electrochemical polymerization; Ionic liquid

* Corresponding author. Tel.: +81-6-6879-7924; fax: +81-6-8679-7875.
E-mail address: yanagida@mls.eng.osaka-u.ac.jp (S. Yanagida).

0010-8545/$ – see front matter © 2004 Elsevier B.V. All rights reserved.
doi:10.1016/j.ccr.2004.03.025

1. Introduction

More than 10 years have passed since dye sensitized solar cells (DSCs) were introduced as next-generation solar cells because of their high efficiency and low production cost [1,2]. The highest conversion efficiency reported for this type of device is more than 10% under AM1.5 (100 mW cm^{-2}) irradiation conditions when liquid electrolytes consisting of liquid I^-/I_3^- redox electrolyte were employed [2]. The use of liquid electrolyte causes several problems such as evaporation or leak of the electrolyte due to difficulty in hermetic sealing. As far as liquid electrolytes are employed, low temperatures may induce crystallization of the iodide salts and high temperatures may enhance the leak of the volatile organic solvent and iodine. Replacing the liquid electrolyte with solid-state hole-transport materials is an essential research subject for improving the long-time stability of the cells. Several attempts have been made to replace the liquid electrolyte with p-type semiconductors [3,4] or organic hole transport materials (HTMs) [5–8]. However, the conversion efficiency of these devices was relatively low particularly under high light irradiance when compared to the liquid electrolyte systems. This may be due to high frequencies of charge recombination to HTMs or poor electronic contact between dye molecules and the HTMs caused by incomplete penetration of solid HTMs in the void of the mesoporous TiO_2 electrodes.

To avoid these problems, we proposed all solid DSCs (sDSCs) using in situ photo-electrochemical polymerization (PEP) of pyrrole as a hole transport phase in the void of the *cis*-Ru^{II} $(L)_2(NCS^-)_2$, (**1**: L = 2,2′-bipyridine-4,4′-dicarboxylic acid; Scheme 1) adsorbed mesoporous TiO_2 electrodes [9]. The in situ polymerization method solves the difficulty in accurate filling of the voids with the semiconductor hole-transport layer, because PPy can be photo-polymerized on the labyrinthine surface of the TiO_2 electrode with the help of the oxidizing ability of the photoexcited dye molecules on the surface.

The use of such in situ polymerized PPy may play a decisive role in the hole transport at the interface between the dye and PPy. It has been shown in the past decade that the dye molecules anchored strongly on the surface of TiO_2 induce extremely fast electron injection within the sub-picosecond time scale, contributing to the effective dye-sensitized charge separation in the solar cells [10–13]. The improved overlap of the HOMO orbital of the dye molecules and conduction band of the hole-transporting semiconductors through chemical interaction is also essential for electron flow at the interface between the dye and the hole transport phase as exemplified by the previous paper [14,15]. Argazzi et al. reported that the ruthenium dye with phenothiazine group, [Ru((4-COO^-)-4′-(COOH)-2,2′-bipyridine)$_2$(4-CH_3-4′-CH_2-phenothiazine-2,2′-bipyridine)] was effective in charge separation due to through-bond hole transfer from the metal center to the phenothiazine group. They also demonstrated that molecular level modification of dyes could tune the dynamics of charge separation and efficiencies in dye-sensitized solar cells [16].

The present review discusses the importance of electronic communication through molecular connection between sensitizing dye molecules and conductive polymers as the hole-transport layer in DSC systems. Novel ruthenium dyes: *cis*-Ru^{II} $(L)_2(pmp)_2$, (**2**: pmp = 3-(pyrrole-1-ylmethyl)-pyridine) [14] and *cis*-Ru^{II} $(L)_2(pp)(solvent)$ (**3**: pp = 4-(1-pyrrolyl)-pyridine; Scheme 1) [15] were successfully synthesized using pyrrole-bearing pyridine ligands. Influence of the pyrrole-bearing ligands on optical and electrochemical properties of the dyed-TiO_2 electrodes was studied. The origin of the sDSC characteristics was discussed based on the effect of pyrrole-bearing pyridine ligands that could work as binding sites of the hole-transporting PPy with the ruthenium metal center of the dye.

In addition, we also successfully fabricated sDSCs using in situ polymerized poly(3,4-ethylenedioxythiophene) (PEDOT) as a hole transport phase [17,18]. PEDOT showed more favorable properties than PPy as an HTM because of high transparency in visible-light range, high conductivity and remarkable stability at room temperature [19]. The influence of the thiophene-bearing ligand molecules on the photovoltaic performance of PEDOT-sDSCs was also examined in view of favorable interaction of HTMs, and sDSC using dye **1** was compared to sDSC using a novel dye: *cis*-Ru^{II} $(L)_2(tp)_2$, (**4**: tp = 4-(2-thienyl)-pyridine; Scheme 1).

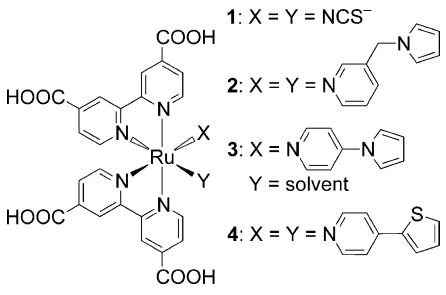

Scheme 1. Chemical structures of synthesized sensitizing ruthenium dyes.

2. Experimental

2.1. Analytical measurements

The purity and structure of the dyes were confirmed by elemental analysis (Perkin-Elmer, 240C), FT-IR spectrum (Perkin-Elmer, System 2000), ES-Mass (Finnigan Mat, TSQ700) and NMR analysis (JEOL, JNM-EX 270 (270 MHz)). The redox potentials of respective dyes were determined by cyclic voltammetry (BAS, 100B/W) in acetonitrile solution containing 0.2 M $LiClO_4$. A working electrode: conducting glass coated F-doped SnO_2 (FTO, Nippon Sheet Glass, 10 Ω/sq.), a reference electrode: Ag^+/Ag (0.01 M), a counter electrode: Pt wire, scan condi-

tion: 0.1 V s^{-1}. The absorption spectra of the dyes were measured using a UV-Vis light spectrometer (Hitachi, U-3000). The HOMO–LUMO energy gap of the dyes was estimated by the absorption threshold of the dye and then potentials of L/L^- were calculated by combining the electrochemical data. The photo-electrochemical properties of the solid cells were studied by recording the current-voltage characteristics under dark conditions or with illumination of AM1.5 (1 Sun, 100 mW cm^{-2}) using a solar simulator (Yamashita Denso, YSS-80). The incident photon-to-current conversion efficiency (IPCE) was also evaluated using a commercial setup for IPCE measurement (JASCO, PV-25DYE) under 5 mW cm^{-2} monochromatic light illumination. The incident light dependent short-circuit currents were measured where the intensity was controlled by a UV cut filter ($\lambda < 390$ nm) and neutral density filters.

2.2. Materials

The ligand L = 2,2′-bipyridyl-4,4′-dicarboxylic acid (dcbpy), $[Ru(L)_2Cl_2]$, $[Ru(L)_2(NCS)_2]$ (**1**) [20] and 4-(1-pyrrolyl)pyridine (pp) [21] were synthesized according to literature procedures. The synthesis of $[Ru(dcbpy)_2(pmp)_2]Cl{\cdot}ClO_4{\cdot}H_2O$ (**2**) was previously described [14]. Pyrrole monomer was purified by vacuum distillation before polymerization. All other chemicals were used as supplied without any further purification.

2.2.1. Synthesis of $[Ru(dcbpy)_2(pp)(EtOH)]ClO_4{\cdot}H_2O$ (*3*)

$Ru(L)_2Cl_2$ (0.5 g, 0.757 mmol) was dissolved in 50 mL of water, and the solution pH was adjusted to 7 by adding NaOH. The solution was evaporated to dryness, and then washed with a mixed solvent of acetone and ether (1:10). The resulting black solid was redissolved in 150 mL of water. The solution was mixed with 150 mL of ethanol containing 0.328 g of pp (2.27 mmol) and then refluxed at 105 °C for 24 h under nitrogen atmosphere. The solution was evaporated, and the resulting reddish brown solid redissolved in 10 mL of water. The solution of 1 M $HClO_4$ was added to give a precipitate that was washed with dilute aqueous HCl (pH = 3), and a mixed solvent of acetone and ether (1:10). A crude brown powder was obtained after drying in vacuum. Purification of the product was carried out as follows. The crude powder was dispersed in 100 mL of water and the solution pH was adjusted to 10 by adding 40% aqueous solution of tetrabutylammonium hydroxide (TBAOH). The solution was stirred for 1 h at room temperature, and then filtered. The resulting solution was evaporated and redissolved in 100 mL of water and passed through a gel permeation column (Sephadex® LH-20) using water as eluent. The resulting solution was evaporated and then dissolved in 20 mL of water. The solution pH was adjusted to 3 by adding of 0.1 M $HClO_4$ and left standing over 100 h. The resulting precipitate powder was extracted with methanol and ethanol, and then reprecipitated with a mixed solvent of acetone and ether (1:10). The resulting powder was redissolved again into 15 mL of ethanol, and was recrystallized in 2 L of ether. A reddish brown powder was obtained after drying in vacuum for 12 h. Elemental analysis for $[C_{35}H_{32}C_{12}N_6O_{18}Ru]$: calcd. (%): C, 42.18; H, 3.24; N, 8.43; found: C, 42.39; H, 3.33; N, 8.78. IR spectrum: 1716, 768, 739 cm^{-1}. ES-mass: found $M_W/n = 390.1$, calcd. $M_W/n = 390.01$. ^{1}H NMR (0.05 M NaOD/D_2O) δ ppm: 9.01 (d, $J = 5.80$ Hz, 1H), 8.97 (d, $J = 5.80$ Hz, 1H), 8.59 (m, 2H), 8.50 (m, 2H), 7.88 (m, 2H), 7.85 (d, $J = 6.10$ Hz, 2H), 7.65 (m, 2H), 7.58 (d, $J = 7.10$ Hz, 2H), 7.41 (m, 2H), 6.31 (d, $J = 6.71$ Hz, 2H), 6.31 (d, $J = 7.10$ Hz, 2H).

2.2.2. Synthesis of 4-(2-thienyl)pyridine

The thiophene-bearing ligand, 4-(2-thienyl)pyridine (tp) was synthesized by Suzuki coupling method based on the previous literature [22]. 4-Bromopyridine hydrochloride (4.86 g, 25 mmol), lithium chloride (3.18 g, 75 mmol), $Pd(PPh_3)_4$ (1.41 g, 1.25 mmol) and 3 M Na_2CO_3 aqueous solution (32.5 mL) were added to distilled toluene (190 mL). An ethanol solution (50 mL) containing 2-thiopheneboronic acid (3.52 g, 27.5 mmol) was added dropwise to the above solution under stirring at 90 °C. After heating this solution for 12 h at 90 °C, the solution was filtered and evaporated, and the resulting precipitate was dissolved in a mixture of diethyl ether and water. The ether extract was dried overnight using magnesium sulfate and then evaporated. The resulting light yellow solid was dried and sublimed at 30 Torr at 70 °C. A transparent colorless solid was obtained by sublimation with yield of 47% (11.75 mmol, 1.89 g).

Anal for $[C_9H_7NS]$, Calcd. (%): C, 67.05; H, 4.38; N, 8.69; S, 19.89. Found: C, 67.28; H, 4.38; N, 8.41; S, 19.62. ^{1}H NMR ($CDCl_3$) δ ppm: 8.57 (dt, 2H), 7.82 (dt, 1H), 7.75 (dt, 1H), 7.65 (dt, 2H) 7.22 (ddd, 1H).

2.2.3. Synthesis of $[Ru(dcbpy)_2(tp)_2]Cl_2$ (*4*)

The synthesized 4-(2-thienyl)pyridine (tp, 245 mg, 1.51 mmol)) was dissolved into 9 mL of DMF, and then $Ru(L)_2Cl_2$ (100 mg, 1.51 mmol) was added to the solution. A microwave oven (microwave oven (SANYO, EM-650T) introduced by a fiber thermometer, 195 W, 2.45 GHz) was used to irradiate the solution under hands-on temperature control for 10 min under a nitrogen atmosphere. The resulting solution was filtered under heating, and then 110 mL of acetone was added to the filtered solution and placed in a refrigerator for 48 h. The resulting precipitate was collected and washed with 50 mL of acetone. A 34 mg of dark brown solid was obtained after filtration and drying. ^{1}H NMR (DMSO) δ ppm: 9.4 (d, 2H), 9.1 (dd, 2H), 9.0 (dd, 2H), 8.67 (d, 4H), 8.25 (dd, 2H), 8.08 (dd, 2H), 7.79 (dd, 4H), 7.61 (m, 6H), 7.20 (t, 2H). Complete purification of the dye could not be achieved even after both re-precipitation and gel permeation column (Sephadex® LH-20) chromatography. ^{1}H NMR revealed that 4% of $Ru(L)_2Cl_2$ remained as an impurity.

2.3. Fabrication of sDSCs combined with PPy

Mesoporous TiO_2 film was fabricated onto a conducting glass electrode (fluorine doped tin oxide, FTO, <10 Ω/sq.) using commercially available TiO_2 powder (P25, Nippon Aerosil) as reported [2]. The TiO_2 electrode was immersed in a 3.0×10^{-4} M dye**1**–**3** in ethanol solution at 60 °C for 50 h in the dark. The electrode was then rinsed with acetonitrile and dried. PPy was introduced into the void of the dye sensitized TiO_2 films by in situ polymerization of pyrrole by the PEP method on the dye sensitized TiO_2 electrode under potentiostatic conditions as reported [14,15]. The potential (+0.1 to −0.3 V) of the dyed films dipped in an acetonitrile solution ($LiClO_4$: 1.0 M, pyrrole: 0.1 M) was maintained by Ag^+/Ag ($AgNO_3$: 0.01 M) reference electrode and then irradiated with a 500 W Xe lamp (22 mW cm^{-2}; λ = 400–800 nm). Total electric charge for anodic photopolymerization was 40 mC cm^{-2}. The TiO_2/dye/PPy electrodes were treated through immersion in an acetonitrile solution of $LiClO_4$ (1.0 M) for 100 h and then washed with acetonitrile and dried to improve the conductivity of the PPy chain by doping of ClO_4^- [9]. We also observed that the adsorption of Li^+ on TiO_2 surface enhances the electron diffusion in mesoporous TiO_2 electrodes [23]. The resulting electrode was clipped with a Pt-sputtered conducting glass to make a solid-state sandwich type DSC.

2.4. Fabrication of sDSCs using PEDOT

A compact TiO_2 layer was deposited on a FTO glass as reported [17] to avoid direct contact between the hole transport phase and the FTO that causes a short circuit in the cell. The mesoporous TiO_2 film was also fabricated in the same way as for the case of sDSCs with PPy. The TiO_2 electrode was immersed in a 3.0×10^{-4} M dye **1** or **4** in ethanol solution at room temperature for 48 h in the dark. The electrode was then rinsed with acetonitrile and dried. The fabrication of sDSCs using in situ chemically polymerized PEDOT (CP-PEDOT) by employing iron(III) tritoluenesulfonate as the oxidizing agent was described elsewhere [17]. PEDOT was also introduced into the void of the dye-adsorbed TiO_2 films by PEP method in the same way as for the case of PPy. (electrolyte: 0.05 M bis(3,4-ethylenedioxythiophene) (bis-EDOT) + 0.1 M $LiClO_4$/acetonitrile.) In this case, EDOT (oxidation potential, E_{OX} ∼ 1.0 V versus Ag^+/Ag) could not be oxidized by the Ru dye in oxidized state (HOMO potential: 0.59 V versus Ag^+/Ag [2]), thus bis-EDOT (E_{OX} ∼ 0.4 V versus Ag^+/Ag) was used as the starting material for polymerization [24]. The polymerization was achieved by applying a constant potential (−0.2 V versus Ag^+/Ag) on the dyed films followed by light irradiation of a 500 W Xe lamp (18 mW cm^{-2}; λ > 520 nm). Total electric charge for anodic photo-polymerization was around 10 mC cm^{-2}. After polymerization, an ionic liquid, 1-ethyl-3-methylimidazolium bis(trifluoromethanesulfone)amide (EMITFSA) solution of 0.2 M lithium bis(trifluoromethanesulfone)amide (LiTFSA) and 0.2 M 4-*tert*-butylpyridine (*t*BP) was cast on the electrode, and left standing for 24 h; the ionic liquid solution on the electrode surface was then wiped off. The resulting electrode was clipped with a gold-sputtered conducting glass to make a sandwich type cell.

3. Results and discussion

3.1. Optical and electrochemical properties of the dyes

Fig. 1 shows the absorption spectra of a 3×10^{-5} M ethanol solution of dyes **1**–**4**. The optical and electrochemical data for the dyes **1**–**4** are also shown in Table 1. The absorption spectra showed blue shifts in the order of **2** > **3** > **4** = **1** depending on the number of pyridine ligands and degree of conjugation of the pyridine ligands. The Ru(III/II) potential for these dyes was also shifted to more positive values with increasing number of pyridine ligands, due to replacement of more strongly donating thiocyanate anions with less donating pyridine ligands [25].

These dyes show almost identical L/L_c potentials and π–π* (λ ∼ 310 nm) absorption bands. The absorption coefficient (ε) of the MLCT absorption band of dye **4** was about half that of dye **1**.

3.2. In situ photo-electrochemical-polymerization of PPy

3.2.1. Polymerization behavior in dye sensitized TiO_2 electrodes

Fig. 2 shows the cyclic voltammograms of dye sensitized TiO_2-electrodes anchoring dye **1**-(a), **2**-(b), and **3**-(c), respectively, which were measured dipped in an acetonitrile solution of $LiClO_4$ (0.2 M) under dark and illumination of visible light (λ = 400–800 nm). Charge transport from the excited state of each dye to the conduction band of TiO_2 was observed when the applied potential reached a negative potential region below about −0.4 V versus Ag^+/Ag. The cyclic voltammograms also revealed that when the applied

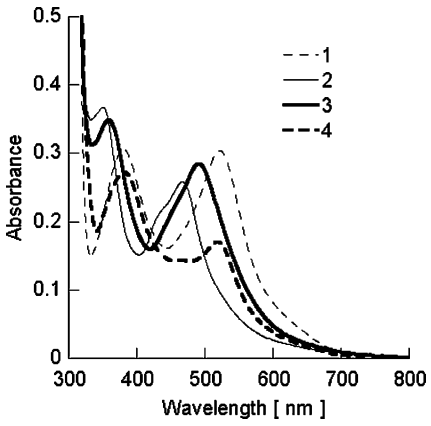

Fig. 1. Absorption spectra of the dyes **1**, **2**, **3**, and **4** in ethanol (3×10^{-5} M).

Table 1
Optical and electrical data for dyes **1**–**4**

	Abs maximum (nm) (ε (10^4 M^{-1} cm^{-1}))	Ru(III/II) (V vs. SCE)	L/L^- (V vs. SCE)
(**1**) $[Ru(L)_2(NCS)_2]$	521 (1.41), 382 (1.42), 310 (5.54)	0.85[a]	−0.90[a]
(**2**) $[Ru(L)_2(pmp)_2]$	466 (1.20), 352 (1.70), 305 (4.39)	0.93	−0.93
(**3**) $[Ru(L)_2(pp)(EtOH)]$	491 (1.32), 359 (1.61), 307 (5.85)	0.98	−0.90
(**4**) $[Ru(L)_2(tp)_2]$	518 (0.79), 382 (1.26), 311 (4.41)	0.89	−0.96

[a] Data obtained from [2].

potential was more positive than +0.2 V versus Ag^+/Ag, polymerization of pyrrole occurs directly on the conducting glass in the presence of pyrrole. Such polymerization of pyrrole causes a short circuit of the device. From these results, the potential on the dye sensitized TiO_2 electrode was applied under control in the range from −0.3 to +0.1 V versus Ag^+/Ag.

To optimize the conditions for the electrochemical polymerization, the effects of the applied potential on the photo-response of the electrodes were investigated using the dye sensitized TiO_2 electrodes. Fig. 3 shows the time course changes of current density during in situ photoelectrochemical polymerization of PPy under various applied potentials for dye **1**-(a), **2**-(b) and **3**-(c) adsorbed TiO_2 electrodes. The polymerization of pyrrole on the dyed film under these conditions proceeds through an initial stage of nucleation followed by diffusion limited polymerization of the monomer [26,27] The peak current densities increased with positive shift of the applied potential in all cases, which corresponds to the fast oxidation and polymerization of pyrrole at higher positive potential. The nucleation time of the electrode polymerized at positive potentials (0, +0.1 V) was relatively longer than the samples polymerized at negative potentials. This longer nucleation time could lead to over-oxidation

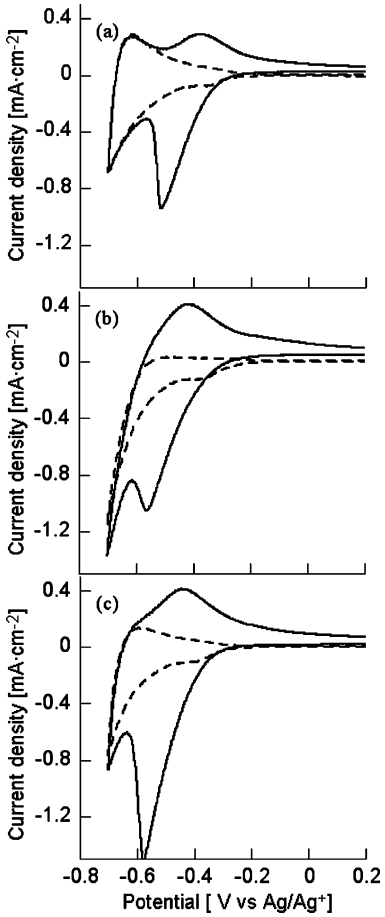

Fig. 2. Cyclic voltammograms of dyed-TiO_2 electrodes: (a) **1**, (b) **2** and (c) **3** in the dark (dashed line) and illumination of 500 W Xe lamp (λ = 400–800 nm, solid line). Measurement condition; solvent: acetonitrile (0.2 M $LiClO_4$), light intensity: 40 mW cm^{-2}, scan rate : 0.1 V s^{-1}.

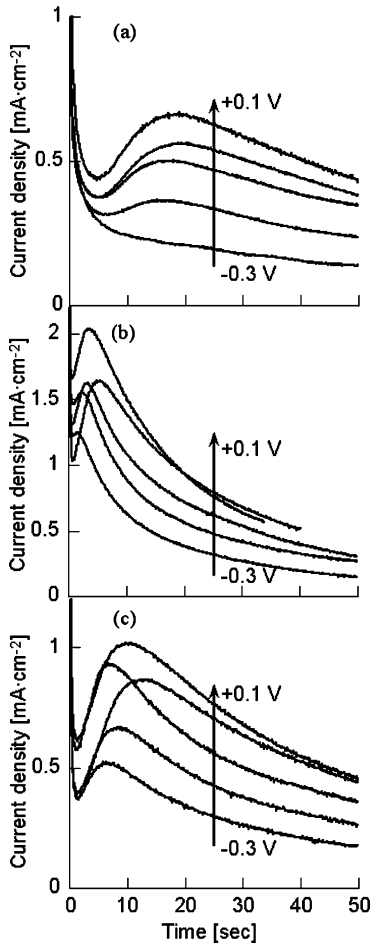

Fig. 3. Current density profile in the polymerization of pyrrole on (a) **1**, (b) **2** and (c) **3** adsorbed TiO_2 electrode with various applied potentials (−0.3/−0.2/−0.1/+0.1 V vs. Ag^+/Ag).

of polypyrrole which provides unfavorable conductivity of polypyrrole. The nucleation process time became shorter with increase in the number of pyridine ligands in the dye. This result suggests that the pyrrole substituent in the pyridine ligand would work as a center of nucleation. The nucleation starting from the pyridine ligand may improve the percolating charge transfer between the dyes and the resultant PPy as expected. This improved charge transport is also supported by the fact that the polymerization current density also increased with the number of pyrrole-bearing pyridine ligands in the dyes at the same applied potential.

3.2.2. Electrochemical behavior for PPy-photodeposited dye sensitized TiO_2 electrodes

Properties of the photodeposited electrodes were evaluated from the photo-associated dope/undoped response of the resulting electrode dipped in an acetonitrile solution (0.4 M) of $LiClO_4$. Fig. 4 shows cyclic voltammograms of TiO_2/dye **1**/PPy polymerized at three different potentials under dark condition or visible light illumination. The total amounts of the electric charge for the polymerization for these electrodes were set to be ca. 40 mC cm^{-2}. Under the dark condition, the Faradaic current due to the reduction of the adsorbed dye molecules as well as the reduction of PPy was observed in the negative potential region below −0.2 V. The charging current due to the capacitance of electrode/electrolyte solution interface became larger as the potential for the deposition becomes positive. The difference in electric charging current should reflect surface roughness of photo-deposited PPy on the dye-adsorbed electrode. This variation of surface roughness depends on the rate of polymerization [28–30]. The photocurrent was found to depend significantly on the polymerization potential. As shown in Fig. 4, the photoresponse in the cyclic voltammogram increased as the polymerization potential becomes negative. The larger photoresponse was observed for the electrodes prepared at negative potentials, which suggests that the electrode polymerized at negative potential shows more effective charge transport from PPy to the excited dye than the electrode polymerized at positive potential. The PPy prepared at a relatively positive potential may be formed rather more randomly than that at the negative potential, giving poor percolation of electron from PPy to the dye sensitized TiO_2. Similar behavior was also observed in both cases of the TiO_2/dye **2** or **3**/PPy electrodes.

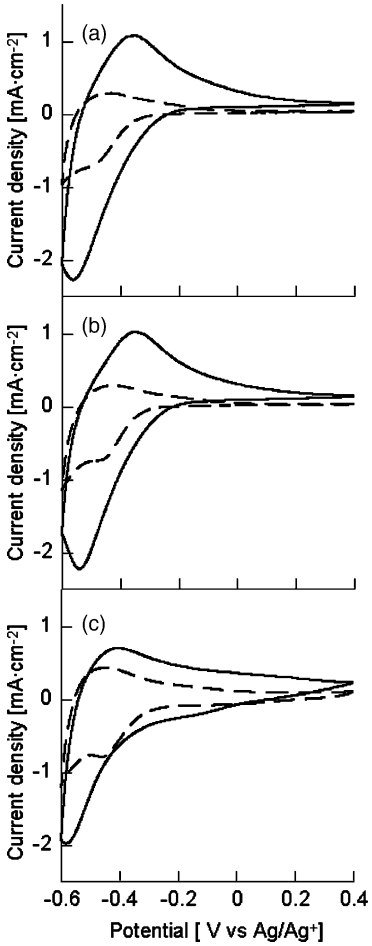

Fig. 4. Cyclic voltammograms of TiO_2/dye **1**/PPy obtained by electropolymerization at potentials of (a) −0.3, (b) −0.1, (c) +0.1 V vs. Ag^+/Ag in the dark (dashed line) and under visible light illumination of 500 W Xe lamp (solid line, light intensity: 50 mW cm^{-2}, λ = 400–800 nm,) in 0.2 M $LiClO_4$ acetonitrile solution.

3.2.3. Photovoltaic performance of PPy polymerized sDSCs

Table 2 lists the performance of solid cells fabricated using the TiO_2/dye **1**, **2** or **3**/PPy electrodes under 10 mW cm^{-2} irradiance (500 W Xe lamp, λ = 400–800 nm). The amount of adsorbed dye was of the same order of 10^{-8} mol cm^{-2}. The highest η for each dye was obtained at a polymerization potential of ca. −0.2 V in good agreement with the good photo-response shown in Fig. 4. The IPCE and absorption

Table 2
Comparison of sensitizing dyes in sDSCs with PPy as HTM and platinum sputtered FTO as counter electrode[a]

Dye	A_{dye} (10^{-8} mol cm^{-2})[b]	E (V)[c]	V_{OC} (V)	J_{SC} (μA cm^{-2})	FF	η (%)
1	7.5	−0.3	0.73	54.0	0.43	0.17
		−0.2	0.75	62.9	0.38	0.18
		−0.1	0.72	65.0	0.32	0.14
		0	0.73	51.6	0.30	0.11
2	6.1	−0.3	0.77	94.7	0.28	0.20
		−0.2	0.78	82.9	0.31	0.20
		−0.1	0.73	67.7	0.37	0.18
		0	0.73	44.3	0.44	0.14
3	6.7	−0.3	0.72	52.5	0.37	0.14
		−0.2	0.75	76.7	0.31	0.18
		−0.1	0.76	57.6	0.37	0.16
		0	0.71	48.7	0.30	0.10

[a] 10 mW cm^{-2} irradiance (500 W Xe lamp, 400–800 nm).
[b] The amount of adsorbed dye on unit projected area.
[c] Applied potential for photo-electro-chemical polymerization of pyrrole.

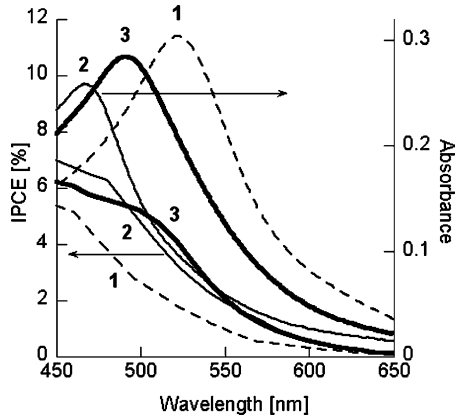

Fig. 5. IPCE spectra of the sDSCs using PEP-PPy sensitized with dye (**1**) (dashed line, polymerization potential: −0.2 V), dye (**2**) (solid line, polymerization potential: −0.3 V) and dye (**3**) (bold line, polymerization potential: −0.2 V), and the absorption spectra of the each dye.

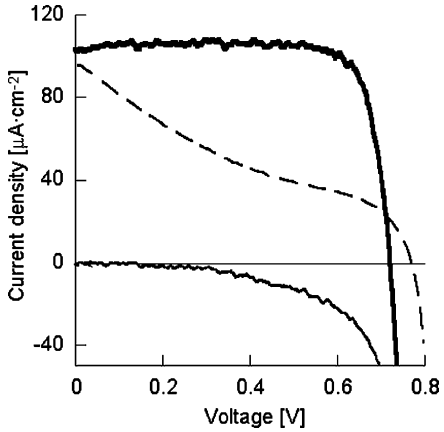

Fig. 6. The photovoltaic performance of the solid-state dye (**2**)-sensitized solar cells with PPy as HTM under 10 mW cm^{-2} light irradiation (500 W Xe lamp, $\lambda = 400$–800 nm): dark (solid line) current and *I–V* curve (bold line) for the cell using a carbon-based counter electrode (polymerization potential: −0.25 V), and *I–V* curve (dashed line) for the cell using a Pt/FTO counter electrode (polymerization potential: −0.3 V).

spectra of the sDSCs using each dye were shown in Fig. 5. Despite the blue shifted absorption bands, the cell fabricated using dye **2** as the sensitizer was the best. This result suggests that the good contact possibly through direct connection between dye and charge transport PPy layer should work effectively to improve the photovoltaic performance of the sDSCs. Interestingly both open circuit voltage (V_{OC}) and short circuit photocurrent density (J_{SC}) were improved by introducing pyrrole-bearing pyridine ligands into the sensitizing ruthenium complexes. The fill factors (FF) of the cells were still low, probably due to the poor charge percolation of PPy layer and poor electric connectivity between PPy and Pt/FTO counter electrode.

To improve the connectivity at the counter electrode, highly conductive carbon-based materials were introduced between PPy and Pt/FTO in the sDSC using dye **2** as a sensitizing dye. A carbon-based paste was prepared by mixing carbon black (Ketjenblack; LION) with an aqueous polydiallyldimethylammonium chloride (PDDAC, 20 wt.% in water, $M_W = 40{,}000$–500,000, Aldrich) solution of 1:6 weight ratio, being spread on the doped TiO_2/dye **2**/PPy electrode. A Pt/FTO electrode was combined together with the TiO_2/dye **2**/PPy/Carbon electrode. They were held by clips and the resulting cell was dried in vacuo for 24 h at room temperature. Fig. 6 shows the best result of the dark and photo *I–V* curves of the solid cells with the carbon-based counter electrode under 10 mW cm^{-2} irradiance. Fig. 6 also shows the photo *I–V* curve of the solid cell only with Pt/FTO as a counter electrode (Table 2: dye **2**, $E = -0.3$ V). The cell with carbon-based electrode showed η of 0.62%, J_{SC} of 104 μA cm^{-2}, V_{OC} of 0.716 V, and FF of 0.78. The η value was six and three times higher than that of the cell with gold [14] and Pt/FTO counter electrodes, respectively. The viscous carbon-based paste on the TiO_2/dye/PPy electrodes provided homogeneous filling in the void of PPy, leading to the improvement of electric connectivity through increased interface of conductive carbon and PPy. The relatively high cathodic dark current of the cell might be explained by back electron transfer from FTO or the dye sensitized TiO_2 to PPy as a recombination process.

3.3. In situ photo-electrochemical polymerization of PEDOT

3.3.1. Influence of the method of polymerization on the cell performance of sDSCs

Fig. 7 shows the *I–V* curves of the sDSCs using in situ chemically polymerized PEDOT under dark and illumination of AM 1.5 conditions. These devices showed lower V_{OC} and FF values than sDSCs with PPy, which could be ascribed to the partial short circuit of the cell arising from the high conductivity of PEDOT. Treatment with EMITFSA significantly improved the dark current property of the cells, which was accompanied by the increase of V_{OC} and FF in pho-

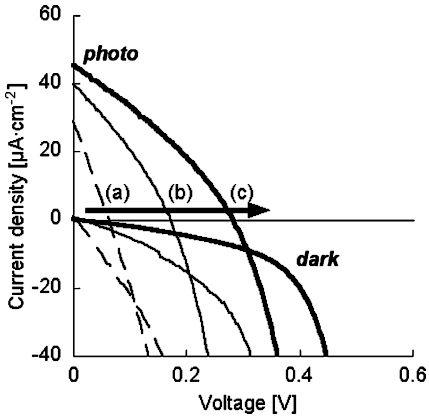

Fig. 7. Effect of EMITFSI on *I–V* characteristics of sDSCs with in situ chemically polymerized PEDOT in the dark and under illumination of AM1.5 light (100 mW cm^{-2}), (a) before treatment, (b) 1 h after treatment and (c) 24 h after treatment.

tocurrent characteristics [17]. The *I–V* characteristics of the cells continued to improve up to about 24 h after treatment (Fig. 7). EMITFSA could form an electrical double layer at the FTO/PEDOT or TiO_2/ PEDOT interfaces, preventing unfavorable contact of the PEDOT at these interfaces which causes electron recombination in the cells. We have also reported that imidazolium cations strongly adsorbed on the TiO_2 surface enhance the electron diffusion in mesoporous TiO_2 electrodes [31,32]. In addition, Lu et al. recently reported that the addition of ionic liquids improved the physical properties of conducting polymers [33]. The addition of LiTFSA and 4-*tert*-butylpyridine (*t*BP) to the EMITFSA solution enhanced the cell performance and the total conversion efficiency (η) reached about twice that of the cell treated only with EMITFSA [17]. The addition of *t*BP and LiTFSA to EMITFSA could also alter this electrical double layer at the TiO_2/PEDOT interface, which would reduce the charge recombination at this interface. Improvement of the photovoltaic performance of solid DSCs using organic HTMs by adding *t*BP and Li salt to HTMs was also reported [6,9]. However, the conversion efficiency of these devices was still very low owing to very poor J_{SC}, which is ascribed to poor connection between the dye molecules on TiO_2 and PEDOT layer and high frequency of charge recombination inside of the DSC.

The treatment of an ionic liquid EMITFSA was also effective for sDSCs using PEP-PEDOT as an HTM. Table 3 shows the photovoltaic characteristics of the dye **1**-sensitized solid cells using PEP-PEDOT, PEP-PPy [15] and CP-PEDOT as the hole transport layer after treatment by EMITFA with LiTFSA and *t*BP [17]. The J_{SC} of sDSCs with PEP-PEDOT was almost 10 times higher than that of CP-PEDOT, which suggests that the PEP method could make better electric contact between dye and HTM than the CP method.

3.3.2. Comparison of PPy and PEDOT as HTMs of sDSCs

When PEDOT was polymerized in dye **1** sensitized TiO_2 using the PEP method, the polymerization current peak (0.05–0.1 mA cm^{-2}) was lower than that of PPy (~0.4 mA cm^{-2}, Fig. 3a). As mentioned in Section 3.2.1, the polymerization current is determined by the nucleation rate and the diffusion rate of the monomer. Taking into account the molecular size, the diffusion rate of bis-EDOT in the voids of porous electrode should be relatively slower compared to that of pyrrole, and may limit the current. However, as shown in Table 3, sDSCs with PEP-PEDOT showed higher J_{SC} than the sDSCs with PEP-PPy whereas the total electric charge for polymerization of PEDOT (~10 mC cm^{-2}) was much lower than that of PPy (~40 mC cm^{-2}). This result could be attributed to the effective excitation of dye molecules due to the high transparency of the resultant PEDOT and better charge transport property of the PEDOT.

Table 3
Comparison of HTMs in sDSCs[a]

HTM	V_{OC} (V)	J_{SC} (mA cm^{-2})	FF	η (%)
PEP-PEDOT	0.56	1.2	0.39	0.26
CP-PEDOT [17]	0.40	0.075	0.37	0.012
PEP-PPy [15]	0.72	0.32	0.78	0.34

[a] Light intensity: 100 mW cm^{-2} (solar simulator, AM1.5).

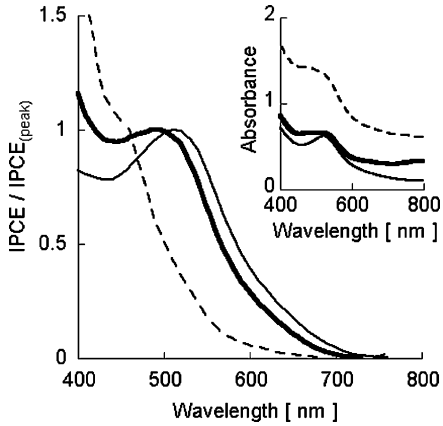

Fig. 8. Normalized IPCE spectra of the liquid DSC (solid line), sDSCs with PEP-PEDOT (bold line), and sDSCs with PEP-PPy (dashed line). Inset: absorbance spectra of the FTO/TiO_2/dye electrode (solid line), FTO/TiO_2/dye/PEP-PEDOT (bold line) and FTO/TiO_2/dye/PEP-PPy(dashed line) (electric charge for polymerization: 10 mC cm^{-2}, dye: $(Bu_4N)_2[Ru(dcbpyH)_2(NCS)_2(N719)]$, TiO_2: Nanoxide-T (Solaronix)).

Fig. 8 shows the normalized IPCE spectra of PEP-PEDOT-sDSC, PEP-PPy-sDSC and of a typical liquid DSC. The shape of the IPCE on PEP-PEDOT-sDSC is similar to that on liquid DSCs, while a lower photoresponse in the visible light range was observed on PEP-PPy-sDSC. Under the same electric charge for polymerization (10 mC cm^{-2}), the increase of absorbance of the dye sensitized electrode after polymerization of PEP-PEDOT was much lower than that of PEP-PPy (see inset of Fig. 8). The better IPCE spectrum of the PEDOT-sDSC is apparently attributable to the better light harvesting efficiency due to the high transparency of PEDOT in the visible region. Fig. 9 shows the light intensity dependent change of the J_{SC} on the sDSCs with PEP-PEDOT and PEP-PPy. The sDSC with PEP-PEDOT shows better linearity between light intensity and J_{SC} than the PEP-PPy-sDSCs. This tendency would be due to the higher conductivity of the PEDOT ($\sigma \sim 400$ S cm^{-1}) [34] compared to that of the PPy (30–120 S cm^{-1}) [35] and due to better connection between PEDOT and dye interface compared to the case of PPy. These results confirm that PEDOT was more suitable than PPy as HTM for fabrication of sDSC in terms of spectral transparency and electronic conductivity. The V_{OC} and FF of the sDSC with PEP-PEDOT were lower than that of the sDSC with PEP-PPy, which could be explained by the unfavorable contact at the TiO_2/dye surface of PEDOT which is more conductive than PPy. The back electron transfer from FTO to PEDOT at FTO/PEDOT interface is also likely a cause of the decrease of the shunt resistance of the cell.

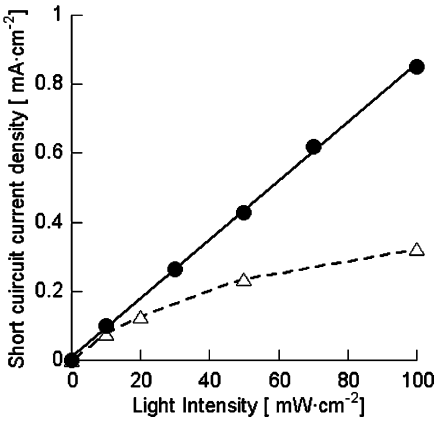

Fig. 9. Dependence of light intensity on short circuit photocurrent density of sDSCs with PEP-PPy (dashed line) and sDSCs with PEP-PEDOT (solid line).

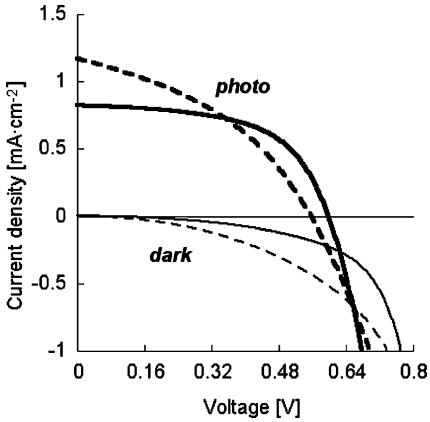

Fig. 11. *I–V* curves of the solid-state dye **1** (dashed line) and dye **4** (solid line) sensitized solar cells using PEP-PEDOT in the dark and under illumination of AM1.5 light (100 mW cm^{-2}).

3.3.3. The effect of a thiophene-bearing ligand in the sensitizing ruthenium dye on the PEP-PEDOT-sDSC

Time course changes in current density during the in situ photo-electrochemical polymerization of PEDOT on the dye **1**- or **4**-adsorbed TiO_2 electrodes are shown in Fig. 10 (polymerization occurs at a potential of −0.2 V versus Ag^+/Ag). The polymerization current on the dye **4**-sensitized electrode showed slower decay than that on the dye **1**-sensitized electrode. Assuming that polymerization of bis-EDOT starts at the thiophene-bearing ligands in the dye **4**, direct covalent bonding between the dye **4** and PEDOT would provide steady and selective tail-end polymerization even when the tail-end is relatively far from the dyed electrode sites. In the case of the diffusion-limited reaction of bis-EDOT, the photo-electrochemical polymerization from the electronically communicating polymer end may result in the steady polymerization of bis-EDOT.

Fig. 11 shows the cell performance of the sDSCs with PEP-PEDOT using dye **1**- or **4**-adsorbed TiO_2 electrodes with dark current. The use of the dye **4** improved the characteristics of V_{OC} (0.56 → 0.60 V), and FF (0.39 → 0.57) of the sDSCs, which could be attributed to the enhancement of charge transport at the dye **4**/PEDOT interface due to the direct connection of the dye with PEDOT as well as the case of PEP-PPy-sDSC. Another explanation is that direct polymerization of PEDOT from the dye **4** could decrease the probability of back electron transfer in PEP-PEDOT-sDSC. On the other hand, J_{SC} of the sDSCs with dye **4** (0.82 mA cm^{-2}) was lower than that of the DSCs with dye **1** (1.2 mA cm^{-2}), resulting in a little improvement of η (0.26 → 0.28%). This is probably due to the low absorption coefficient (ε) of the dye **4** compared to the dye **1** (see Table 1). Direct evidence for a connection between the dye and HTMs has not yet been obtained. The confirmation of this chemical connection is in progress. More appropriate molecular design of the sensitizing Ru complexes that have both adequate ε and thiophene-bearing ligands which are reactive in photo-electropolymerization will lead to improved photovoltaic performance of the sDSCs.

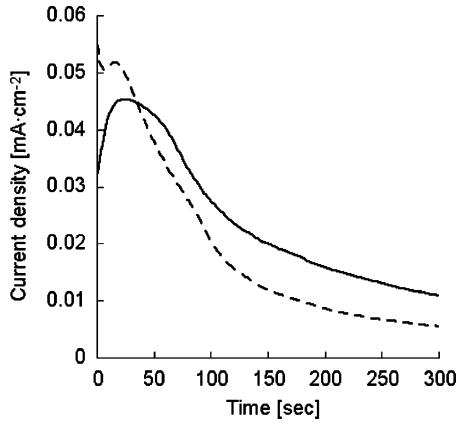

Fig. 10. Polymerization current density profile of PEP-PEDOT in dye **1** (dashed line) and dye **4** (solid line) adsorbed TiO_2 electrode. (the applied potential: −0.2 V vs. Ag^+/Ag).

4. Conclusion

All-solid state dye sensitized solar cells were successfully fabricated using in situ polymerized conducting polymers, PPy or PEDOT, as the hole transport phase in place of liquid electrolytes. Combination of the in situ polymerization with novel ruthenium dyes which have pyrrole or thiophene units in the ligand system improved the photovoltaic performance of the solid DSCs. The effect of these ligands can be explained through the improved charge transport at the interface of the sensitizing dye molecules and the HTMs. The use of a carbon-based counter electrode and treatment of the polymer phase with an ionic liquid also improved the cell performance of the sDSCs. These effects could be attributed to the enhancement of charge transport property at HTMs/counter electrodes and mesoporous-TiO_2/HTMs interface, respectively. These results will contribute to molecular level management of the charge transport occurring at

every interface such as dye/HTM, HTM/counter electrode, TiO_2/HTM, which is essential to improve the performance of sDSCs.

Acknowledgements

The authors wish to acknowledge H.C. Stalk V TECH Ltd. for kindly supplying the 3,4-ethylenedioxythiophene. This work was partially supported by Open Competition for the Development of Innovative Technology (No. 12310) in Grant-in-Aid for the Creation of Innovations through Business-Academic-Public Sector Cooperation from the Ministry of Education, Culture, Sports, Science and Technology of Japan, and by the Strategic Research Base, Frontier Research Center, (Graduate School of Engineering) Osaka University, supported by the Japanese Government's Special Coordination Fund for Promoting Science and Technology.

References

[1] B. O'Regan, M. Grätzel, Nature London 353 (1991) 737.
[2] M.K. Nazeeruddin, A. Kay, I. Rodicio, R. Humphry-Baker, E. Mueller, P. Liska, N. Vlachopoulos, M. Grätzel, J. Am. Chem. Soc. 115 (1993) 6382.
[3] K. Tennakone, G.R.R.A. Kumara, I.R.M. Kottegoda, K.G.U. Wijayantha, V.P.S. Perera, J. Phys. D Appl. Phys. 31 (1998) 1492.
[4] B. O'Regan, D.T. Schwartz, S.M. Zakeeruddin, M. Grätzel, Adv. Mater. 12 (2000) 1263.
[5] U. Bach, D. Lupo, P. Comte, J.E. Moser, F. Weissörtel, J. Salbeck, H. Spreitzer, M. Grätzel, Nature 395 (1998) 583.
[6] J. Krüger, R. Plass, L. Cevey, M. Piccirelli, M. Grätzel, U. Bach, Appl. Phys. Lett. 79 (2001) 2085.
[7] J. Krüger, R. Plass, M. Grätzel, H.-J. Matthieu, Appl. Phys. Lett. 81 (2002) 367.
[8] D. Gebeyehu, C.J. Brabec, N.S. Sariciftci, D. Vangeneugden, R. Kiebooms, D. Vanderzande, F. Kienbeerger, H. Schindler, Synth. Met. 125 (2002) 279.
[9] K. Murakoshi, R. Kogure, Y. Wada, S. Yanagida, Chem. Lett. 5 (1997) 471.
[10] J.M. Rehm, G.L. McLendon, Y. Nagasawa, K. Yoshihara, J. Moser, M. Grätzel, J. Phys. Chem. 100 (1996) 9577.
[11] Y. Tachibana, J.E. Moser, M. Grätzel, D.R. Klug, J.R. Durrant, J. Phys. Chem. 100 (1996) 20056.
[12] R.J. Ellingson, J.B. Asbury, S. Ferrere, H.N. Ghosh, J.R. Sprague, T. Lian, A.J. Nozik, J. Phys. Chem. B 102 (1998) 6455.
[13] G. Benkö, J. Kallioinen, J.E.I. Korppi-Tommola, A.P. Yartsev, V. Sundström, J. Am. Chem. Soc. 124 (2002) 489.
[14] K. Murakoshi, R. Kogure, Y. Wada, S. Yanagida, Sol. Energy Mater. Sol. Cells 55 (1998) 113.
[15] T. Kitamura, M. Maitani, M. Matsuda, Y. Wada, S. Yanagida, Chem. Lett. 9 (2001) 1054.
[16] R. Agrazzi, C.A. Bognozzi, T.A. Heimer, F.N. Castellano, G.J. Meyer, J. Am. Chem. Soc. 117 (1995) 11815.
[17] Y. Saito, T. Kitamura, Y. Wada, S. Yanagida, Synth. Met. 131 (2002) 185.
[18] Y. Saito, N. Fukuri, R. Senadeera, T. Kitamura, Y. Wada, S. Yanagida, Electrochem. Commun. 6 (2004) 71.
[19] L.B. Groenendaal, F. Jonas, D. Freitag, H. Pielartzik, J.R. Reynolds, Adv. Mater. 12 (2000) 481.
[20] M.K. Nazeeruddin, S.M. Zakeeruddin, R. Humphry-Baker, M. Jirousek, P. Liska, N. Vlachopoulos, V. Shklover, C.-H. Fischer, M. Grätzel, Inorg. Chem. 38 (1999) 6298.
[21] M.J. Atkins, D.J. Harwood, R.B. Lowry, Inorg. Chim. Acta 244 (1996) 277.
[22] V. Percec, J.-Y. Bae, D.H. Hill, J. Org. Chem. 60 (1996) 1060.
[23] S. Nakade, S. Kambe, T. Kitamura, Y. Wada, S. Yanagida, J. Phys. Chem. B 105 (2001) 9150.
[24] G.A. Sotzing, J.R. Reynolds, P.J. Steel, Adv. Mater. 9 (1997) 795.
[25] A.B.P. Lever, Inorg. Chem. 29 (1990) 1271.
[26] E.M. Genies, G. Bidan, A.F. Diaz, J. Electroanal. Chem. 149 (1983) 101.
[27] S. Asavapiriyanont, G.K. Chandler, G.A. Gunawardena, D. Pletcher, J. Electroanal. Chem. 177 (1984) 245.
[28] R. Stankovicc, O. Pavlovic, M. Vojnovic, S. Jovanovic, Eur. Polym. J. 30 (1994) 385.
[29] R.C.D. Peres, J.M. Pernaut, M.-A.D. Paoli, J. Polym. Sci. A Polym. Chem. 29 (1991) 225.
[30] M. Satoh, K. Kaneto, K. Yoshino, Synth. Met. 14 (1986) 289.
[31] S. Kambe, S. Nakade, T. Kitamura, Y. Wada, S. Yanagida, J. Phys. Chem. B 106 (2002) 2967.
[32] W. Kubo, S. Kambe, S. Nakade, T. Kitamura, K. Hanabusa, Y. Wada, S. Yanagida, J. Phys. Chem. B 107 (2003) 4374.
[33] W. Lu, A.G. Fadeev, B. Qi, E. Smela, B.R. Mattes, J. Ding, G.M. Spinks, J. Mazurkiewicz, D. Zhou, G.G. Wallace, D.R. MacFarlane, S.A. Forsyth, M. Forsyth, Science 297 (2002) 983.
[34] P.-H. Auberta, L. Groenendaal, F. Louwet, L. Lutsen, D. Vanderzande, G. Zotti, Synth. Met. 126 (2002) 193.
[35] M. Brie, R. Turcu, A. Mihut, Mater. Chem. Phys. 49 (1997) 174.